Construction and Building Materials 141 (2017) 315–324

Contents lists available at ScienceDirect

Construction and Building Materials

journal homepage: www.elsevier.com/locate/conbuildmat

Stepwise regression modeling for compressive strength of alkali-activated concrete

R.J. Thomas [a], Sulapha Peethamparan [b,*]

[a] Dept. of Civil and Environmental Engr., Utah State University, Logan, UT, USA
[b] Dept. of Civil and Environmental Engr., Clarkson University, Potsdam, NY, USA

HIGHLIGHTS

- Compressive strength of alkali-activated fly ash and slag concrete is tested.
- Effects of various mixture parameters are quantified.
- Predictive models for compressive strength are developed.

ARTICLE INFO

Article history:
Received 30 November 2016
Received in revised form 9 February 2017
Accepted 1 March 2017
Available online 10 March 2017

Keywords:
Alkali-activated concrete
Compressive strength
Strength modeling
Fly ash
Slag cement

ABSTRACT

This paper presents the results from a parametric experimental investigation of the compressive strength of alkali-activated concrete. The effects of curing condition (moist-cured versus heat-cured), sodium oxide dosage, silica dosage, silica modulus (relative dosage of silica to sodium), solution/binder ratio, and free water/binder ratio on the compressive strength of sodium silicate-activated fly ash and slag cement concrete are evaluated. More than 5000 specimens with 676 unique combinations of mixture proportion and curing condition were tested. The marginalized effects of each parameter indicate effects similar to those identified by previous studies. Predictive models for the compressive strength of fly ash and slag cement-based concretes are developed by stepwise regression analysis. Although the specific models presented in this paper are applicable only for the materials and activators identified herein, the modeling procedures are generalized results are of doubtless utility for the design of alkali-activated concrete mixtures.

1. Introduction

Alkali-activated concrete is made by the chemical activation of aluminosilicate materials with strong metal alkalis. Activators like sodium or potassium hydroxide, sodium silicate, or sodium carbonate are commonly used in conjunction with industrial byproducts like fly ashes or slag cement to produce strong and durable binders. Although alkali-activation of aluminosilicates dates back to at least 1908 [1], alkali-activated concretes (AAC) have only recently emerged as potential replacements for portland cement concrete. The recent emergence of AAC stems mainly from increased concern over the environmental impact of portland cement manufacture. The embodied energy and carbon emissions associated with AAC are significantly lower than those associated with portland cement concrete (PCC) [2–4].

The compressive strength behavior of alkali-activated binders has been discussed at length in existing literature. The compressive strength of alkali-activated slag cement (AASC) is known to be influenced by binder composition, activator composition and concentration, water content, and curing condition. Several researchers have suggested that the optimal strength performance in AASC is obtained when sodium silicate is used as the activator [5–9]. The compressive strength is known to increase as the alkali concentration of the activator increases and as the ratio of silica to sodium oxide increases [5–12]. The compressive strength is known to decrease as the water/binder or solution/binder ratio increases, given sufficient water for adequate workability and consolidation [5]. The accelerating effect of heat-curing on strength gain in AASC concrete has been often reported [5,6,13–16]. [6] suggest that temperature is second only to activator concentration in terms of its effect on compressive strength. Additionally, the compressive strength of AASC concrete tends to increase with binder content [17].

* Corresponding author.
E-mail addresses: thmsrj@gmail.com (R.J. Thomas), speetham@clarkson.edu (S. Peethamparan).

http://dx.doi.org/10.1016/j.conbuildmat.2017.03.006
0950-0618/

Similarly, the compressive strength of alkali-activated fly ash (AAF) concrete is known to vary with the composition of the binder, the composition and concentration of the activator, the water content, and the curing condition [18–26]. Extremely high compressive strengths, in the range of 70–100 MPa, have been achieved in AAF binders with very high alkali concentrations or elevated temperature [5,22,27,28]. Several studies have suggested an optimum silica modulus near 1.5 for AAF concrete when sodium silicate is used as the activator [25,26,29,30].

Despite the wealth of research describing the compressive strength behavior of alkali-activated binders and concrete summarized above, there have been few attempts to model the compressive strength as a function of the mixture parameters (e.g., activator concentration, water content). [6] presented some basic categorical models for the compressive strength of AAS concrete. [31] modeled the compressive strength of potassium hydroxide-activated natural pozzolans, which was based on chemical composition, alkali solubility, and pozzolan crystallinity. [32] evaluated various methods of predicting the compressive strength of AAF concrete. Those methods varied in reliability, but focused mainly on the physical and chemical properties of the binders as predictors of strength. Suggesting that it will be of more use to practitioners to predict the compressive strength of AAC made with a given binder based on mixture parameters, the present study purports to model the compressive strength of sodium silicate-activated fly ash and slag cement concrete as a function of activator composition, water content, and curing condition. Specifically, the effects of sodium oxide dosage, silica dosage, silica modulus (relative concentration of silica to sodium oxide), solution-to-binder ratio, free water-to-binder ratio are investigated for AAF and AASC concretes cured at ambient temperature (moist-cured at 23 °C for 28 d) and elevated temperature (heat-cured at 50 °C for 48 h).

2. Experimental

2.1. Materials

The binder materials were class C fly ash and slag cement. The former was sourced from the Belle River Power Plant, a subsidiary of Detroit Edison in St. Clair County, MI. The latter was sourced from Holcim USA at the Chicago Skyway Plant in Chicago, IL. The chemical composition is given in Table 1.

The activator was a compound aqueous solution of sodium silicate and sodium hydroxide. The sodium oxide dosage N and silica dosage S were specified by percent mass of binder. The silica modulus m is the mass ratio of silica to sodium oxide, $m = S/N$. Solutions were prepared by mixing deionized water, sodium oxide pellets, nanosilica powder, and a commercial sodium metasilicate solution in the prescribed ratios. The solution-to-binder ratio s is the mass ratio of activator solution to binder, and the free water-to-binder ratio w is the mass ratio of water in the activator solution to binder.

The fine aggregate was quartz sand with specific gravity 1.91 and fineness modulus 2.54. The coarse aggregate was quarried crushed stone composed predominately of pink limestone. The maximum aggregate size was 13 mm.

2.2. Mixture proportioning and parameters

This study evaluated the effects of several mixture parameters. Mixture proportions were computed according to the absolute volume method with bulk volume of coarse aggregate of 0.5 [33]. Binder type was either fly ash or slag cement as previously described. The curing condition was either moist-curing (23 ± 2 °C for 28 d) or heat-curing (50 ± 0.1 °C for 48 h). This heat-curing regime was selected because it has been commonly used throughout the literature, and is the minimal temperature that will result in at least the same strength in 48 h as under moist-curing for 28 d [26,34,35]. The sodium oxide dosage N, silica dosage S, silica modulus m, the solution-to-binder ratio s, and the free water-to-binder ratio w were also varied. It should be noted that this shorthand nomenclature is somewhat nonstandard but has been adopted for the sake of brevity and clarity.

The range of parameters evaluated for each binder type is listed in Table 2. Activator compositions are typically specified by sodium oxide dosage N, silica modulus m, and solution-to-binder ratio s. As such, the silica dosage S and free water-to-binder ratio w were not directly varied. Quantification of the effect of these parameters was, however, still of interest. Based on preliminary experimentation [36], it was determined that mixtures with $w < 0.3$ were insufficiently workable. Additionally, mixtures with $S < 1$ were deemed unfairly representative of the behavior of the compound activator. The intermediate values $N = \{4.2, 4.4, 4.6, 4.8\}$ were included for AAF concrete based on preliminary investigations which suggested a sharp rise in strength between sodium oxide dosages of 4 and 5% [36].

2.3. Experimental methods

AAC mixtures were prepared in a standard bench top laboratory mixer. The binder and saturated surface dry aggregates were first charged into the mixing bowl and mixed for 60 s. The activator solution, prepared at least 24 h in advance of mixing, was charged into the mixing bowl over the course of 30 s with the mixer running at low speed. The batch was then mixed at medium speed for an additional two minutes. Following mixing, concrete was immediately cast into ϕ76.2 × 152.4 mm cylinders and consolidated by mechanical vibration. Reagent-grade activators were used to keep precise control over the activator composition; the costs associated with these activators necessitated the use of specimens smaller than the standard ϕ152.4×304.8 mm cylinders. Each specimen was sealed with plastic and placed in the prescribed curing condition. Eight specimens were cast from each batch; four were placed in each curing condition. Each batch was cast in two replicates; a total of 646 total batches and 5168 total specimens were

Table 1
Binder composition.

	Slag cement	Fly ash
	(mass percent)	
SiO_2	36.0	37.7
Al_2O_3	10.5	20.0
CaO	39.8	23.4
MgO	7.9	4.3
Na_2O	0.3	1.7
SO_3	2.1	2.4
K_2O	0.2	0.6
Fe_2O_3	0.7	5.6
LOI	0.00	0.31

Table 2
Mixture proportion variables, ranges, and restrictions.

Binder:	Fly ash C	Slag cement
Curing	Moist-cured, heat-cured	Moist-cured, heat-cured
N	2, 3, 4, 4.2, 4.4, 4.6, 4.8, 5, 6, 7	1, 2, 2.5, 3, 3.5, 4, 4.5, 5, 5.5, 6, 7
m	0.5, 1, 1.5, 2.5	0.5, 0.75, 1, 1.5, 2.5, 3.5
S	⩾1.0	⩾1.0
s	0.35, 0.4, 0.425, 0.45, 0.5	0.35, 0.4, 0.425, 0.45, 0.5
w	>0.3	>0.3

cast over a period of more than one year. Specimens remained sealed in their molds for the entire curing duration and were tested within one percent of the prescribed duration. Compressive strength was determined in accordance with the specifications of ASTM C192 using a hydraulic compression tester of capacity 1.1 MN. Each reported strength value is the average of four replicate specimens.

3. Analytical

Predictive models were developed by stepwise regression using `stepwiselm` in MATLAB. Stepwise regression analysis is an algorithmic approach to model selection that can be accomplished by forward selection or backward elimination. Under the former, a constant model is selected and model terms of increasing complexity are added until the fit is optimized. Under the latter, a highly complex model is selected, and model terms are removed until the fit is optimized. The choice of which term is added or removed in each step is based on that which most improves the fit, as evaluated by some specified model criterion. In this study, the Bayesian Information Criterion,

$$\mathrm{BIC} = k \ln n - 2\hat{\ell}, \tag{1}$$

is used as the model criterion, where k is the number of free model parameters, n is the sample size, and the log-likelihood ℓ. The log-likelihood ℓ is the natural logarithm of the likelihood function $\mathcal{L}$, which is defined as the probability of observing the data x from a population X given the model θ:

$$\mathcal{L} = P(X = x|\theta). \tag{2}$$

The model fit is optimized by minimizing BIC. BIC was selected as the model criterion because it heavily penalizes for overfitting. Overfitting describes the tendency to select a model of high order which naturally fits the data better but may be much less economical. The null value hypothesis test and the associated p-value is not used for reasons discussed elsewhere [37,38] Separate models were developed for the compressive strength of AAF and AASC concrete. Curing condition was treated as a categoric variable; the resulting models include a boolean term T which is equal to zero if moist-cured and 1 if heat-cured. The remaining variables were treated as numeric.

4. Results and discussion

The compressive strength results for sodium silicate-activated fly ash and slag cement concrete are presented in this section. Compressive strengths in the range 1.0–55 MPa were observed for moist-cured AAF concrete; values in the range 0.9–77 MPa were observed for heat-cured AAF concrete. The population standard deviation for the compressive strength of all AAF concrete specimens was 16.5 MPa. The average sample standard deviation from each group of four specimens was 1.13 MPa, or about 6% of the average strength from each group of four. Compressive strength in the range 0.1–83 MPa were observed for moist-cured AASC concrete; values in the range 1.2–88 MPa were observed for heat-cured AASC concrete. The population standard deviation for the compressive strength of all AASC concrete specimens was 18.6 MPa. The average sample standard deviation from each group of four specimens was 1.39 MPa, or about 4% of the average strength from each group of four. The effects of the aforementioned mixture parameters are discussed below.

4.1. Marginalized results

This section presents the compressive strength results marginalized by each factor (i.e., the compressive strength as a function of a single factor without regard for the other factors). This shows the general effect of each individual parameter and provides a basis for comparison of the dataset with previously published results. The marginalized effects of sodium oxide dosage N, silica dosage S, silica modulus m, solution-to-binder ratio s, and free water-to-binder ratio w on the compressive strength of AAF and AASC concrete are shown in Figs. 1–5. The effect of curing condition on the compressive strength of these mixtures has been discussed elsewhere [35] and will not be discussed in detail here. It is important to note here that the discussion of marginalized results is not included for the prediction of compressive strength. Instead, it is presented simply to show what general trends may be observed in the data.

The effect of sodium oxide dosage N on compressive strength f'_c is shown in Fig. 1. Recall that the figure shows that marginalized results for compressive strength as a function of sodium oxide dosage. Within a single sodium oxide dosage, all other parameters vary throughout their entire ranges. This figure, and the others that follow, can be interpreted to give two types of information. First, the figure shows the general trend of compressive strength as a function of sodium oxide dosage without regard for the value of other parameters. Second, the figure shows the range of strengths that can be expected at a particular sodium oxide dosage. For example, the compressive strength of AASC concrete (Fig. 1b) with $N = 2.5$ can range from 10 to 60 MPa with varying combinations of silica dosage and other parameters.

Consistent with existing literature, the result presented in Fig. 1 suggest increased compressive strength with increased sodium oxide dosage within the range tested ($N \leq 7\%$). Some researchers have suggested an optimum activator concentration, above which the compressive strength may decrease [29,30,25,26]. The compressive strength observations for AAF concrete are somewhat consistent with this idea. Although no decrease in compressive strength was observed, the strength-increasing effect of increased sodium oxide dosage was markedly decreased above about 5%. No such decrease was observed for AASC concrete; instead, the compressive strength tended to increase approximately linearly with sodium oxide dosage through the range $1\% \leqslant N \leqslant 7\%$.

Similarly, the effect of silica dosage S on compressive strength f'_c is shown in Fig. 2. AASC concrete exhibited a clearly observable increase in compressive strength with silica dosage throughout the range $0.5\% \leqslant S \leqslant 14\%$. This increase was steady for silica dosages up to about $S = 4\%$ and far less significant above that value. This is again somewhat consistent with previous studies which have suggested optimum activator concentrations from the standpoint of compressive strength. In the case of AAF concrete, the marginalized effect of silica dosage was unclear. There was a general increasing trend in compressive strength with silica dosage, but the rate of increase was highly variable. While silica dosage could be used as a rough predictor for the compressive strength of AASC concrete, it is without question that the same cannot be said for AAF concrete.

The effect of silica modulus m on compressive strength f'_c is shown in Fig. 3. A wide range of compressive strengths was observed at each silica modulus for both AAF and AASC concrete, suggesting that a reasonable prediction of compressive strength cannot be made from the silica modulus alone. However, an optimum silica modulus from the standpoint of compressive strength was apparent in both AAF and AASC concrete, although much more so in the latter. The optimum was near $m = 1.5$ for both.

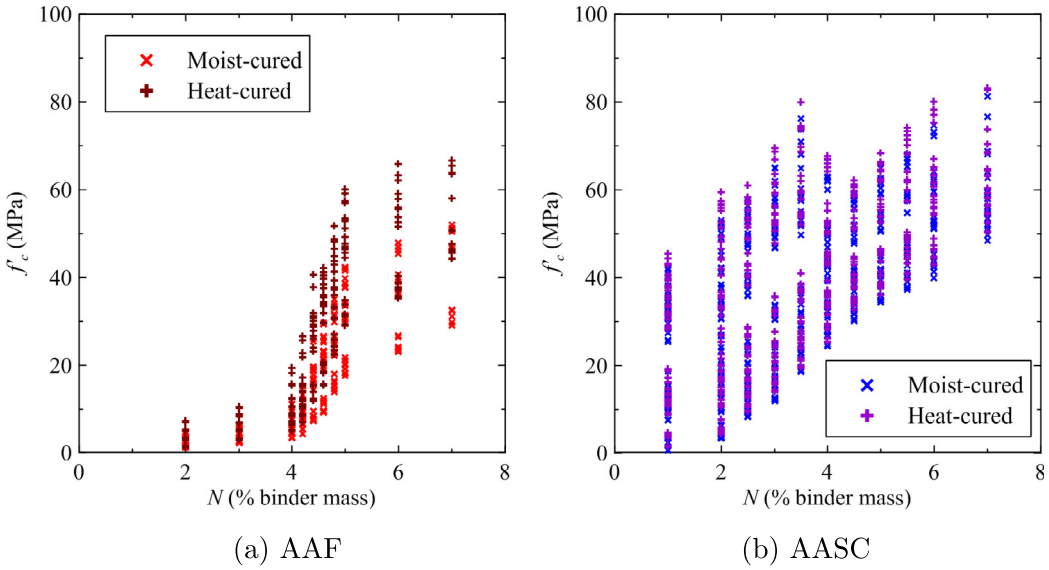

Fig. 1. Compressive strength f'_c vs. sodium oxide dosage N (% binder mass).

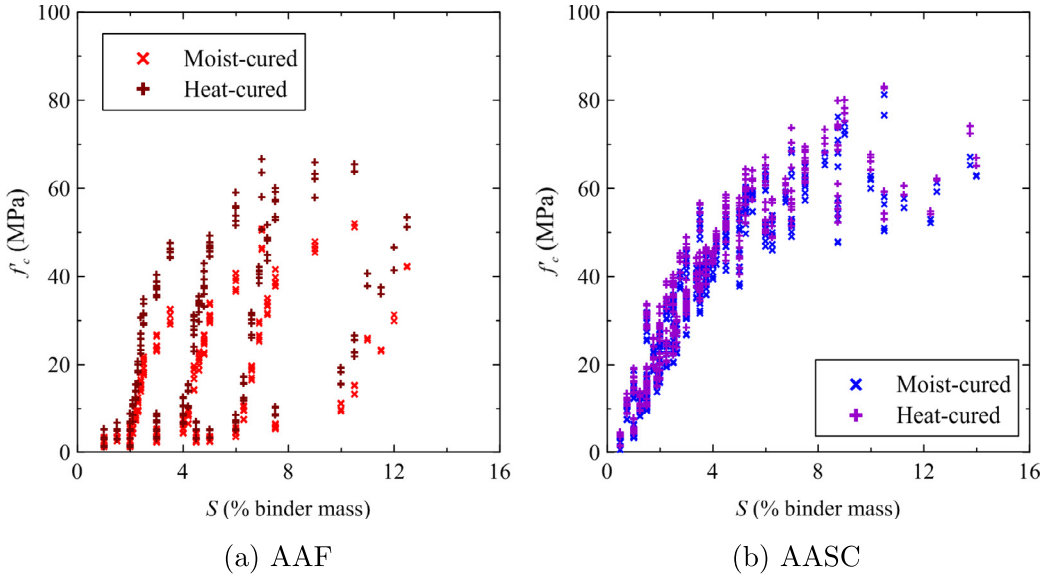

Fig. 2. Compressive strength f'_c vs. silica dosage S (% binder mass).

The effects of solution-to-binder ratio s and free water-to-binder ratio w on compressive strength f'_c are shown in Figs. 4 and 5, respectively. In both cases, the range of compressive strengths observed at each value is wide, and neither could reasonably be used as a sole predictor of compressive strength. However, the expected overall decrease in compressive strength with increased free water-to-binder ratio w is observed in Fig. 5. The same expected result is not observed for solution-to-binder ratio s in Fig. 4. The data plotted in that figure are somewhat misleading, however, due to the constraints on free water-to-binder ratio in Table 2 (i.e., $w > 0.3$). The minimum solution-to-binder ratio used in the parametric study was 0.35. Considering the constraint on free water-to-binder ratio, that value was only valid for activator solutions with low alkali content. Higher solution-to-binder ratios allowed higher alkali contents, which led to higher overall compressive strengths (as demonstrated in Figs. 1–3). With that in mind, there was no observable trend in compressive strength as a function of solution-to-binder ratio.

4.2. Predictive models

The previous section demonstrates that the observed compressive strength data are in overall agreement with the literature, which serves as some evidence of their validity. This section presents several mathematical models for the prediction of compressive strength based on the parameters discussed above. Thousands of predictive models were evaluated by the `stepwiselm` algorithm. The goal was to produce the simplest model that could adequately describe the desired effects. To that end, several classes of models were considered. These were (in increasing order of complexity):

1. Linear without interactions
2. Linear with second-order interactions
3. Quadratic without interactions
4. Quadratic with second-order interactions
5. Cubic with third-order interactions

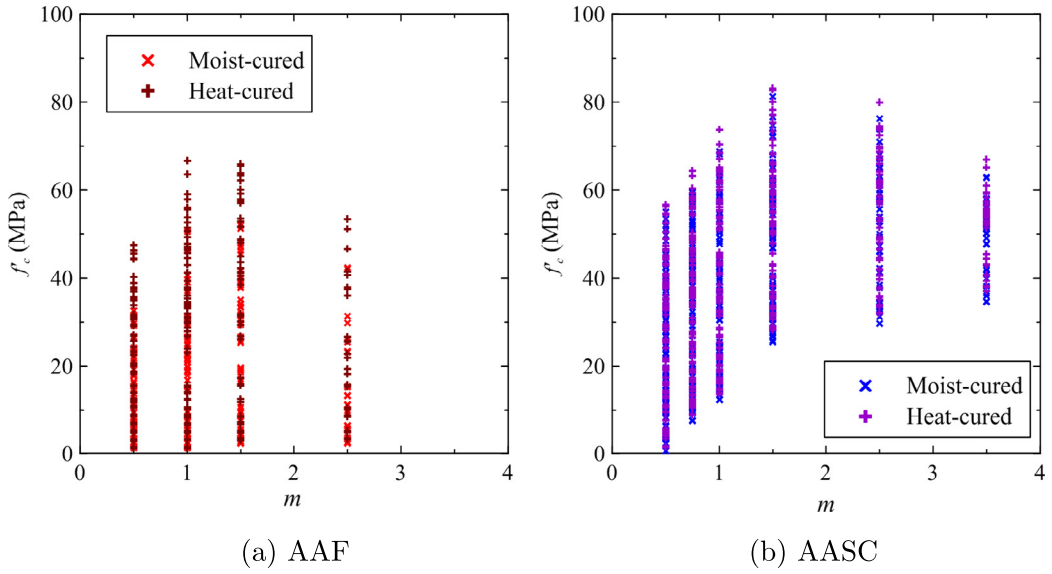

Fig. 3. Compressive strength f'_c vs. silica modulus m.

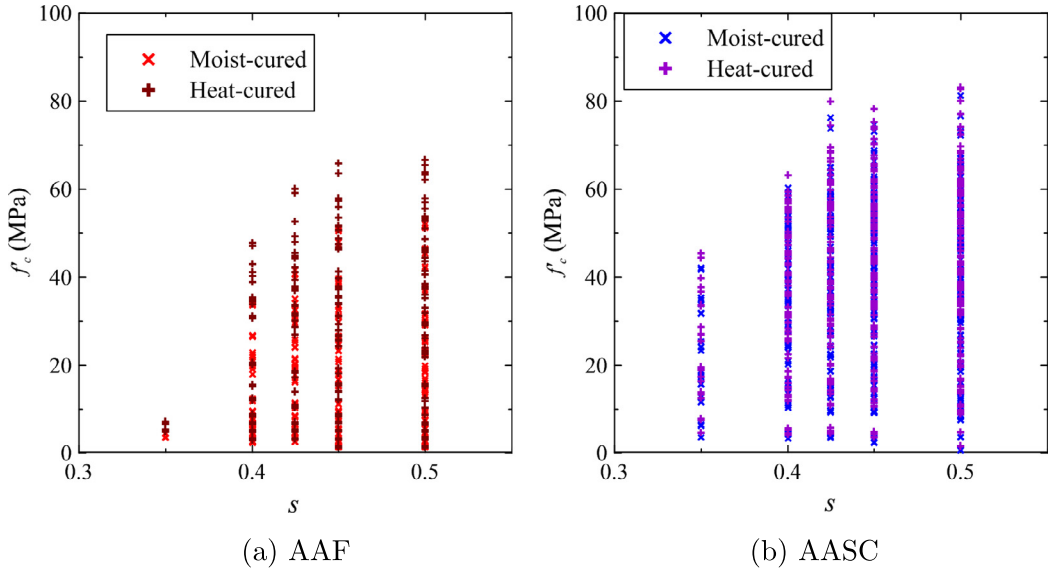

Fig. 4. Compressive strength f'_c vs. solution-to-binder ratio s.

The optimal model from each class is discussed in this section.

4.2.1. AAF concrete

The optimal predictive models of classes 1–5 for the compressive strength of AAF concrete are presented as Eqs. (3)–(7). All of the models of increasing complexity include intercept terms and terms for curing condition, sodium oxide dosage, silica dosage, and silica modulus. Researchers commonly describe sodium silicate concentrations using the sodium oxide dosage and the silica modulus, which is an adequate description of the activator composition. Based on this convention, it was assumed from the conception of this study that those two terms would also be adequate for prediction of compressive strength. The results shown here suggest otherwise. The coefficient on T was identical between model Eqs. (3) and (5) and between model Eqs. (4) and (6). This suggests that the effect of curing condition can be modeled with reasonable certainty, which is consistent with conclusions presented elsewhere [35].

All of the aforementioned models except Eq. (4) include terms for the solution-to-binder ratio, while Eq. (4) includes terms for free water-to-binder ratio. None of the equations include terms for both s and w. This suggests that only one term describing the water content is necessary for accurate strength prediction, and that the solution-to-binder ratio likely provides a better prediction.

$$f'_c = -5.514 + 7.581T + 7.337N + 3.514S - 6.539m - 40.26w \quad (3)$$

$$f'_c = 6.227 - 6.930T + 2.705N - 4.818S + 10.55m - 37.57s + 3.500TN + 1.524NS - 0.8886mS \quad (4)$$

$$f'_c = 26.29 + 7.581T - 10.07N + 8.730S - 16.51m - 36.68s + 1.729N^2 - 0.2249S^2 \quad (5)$$

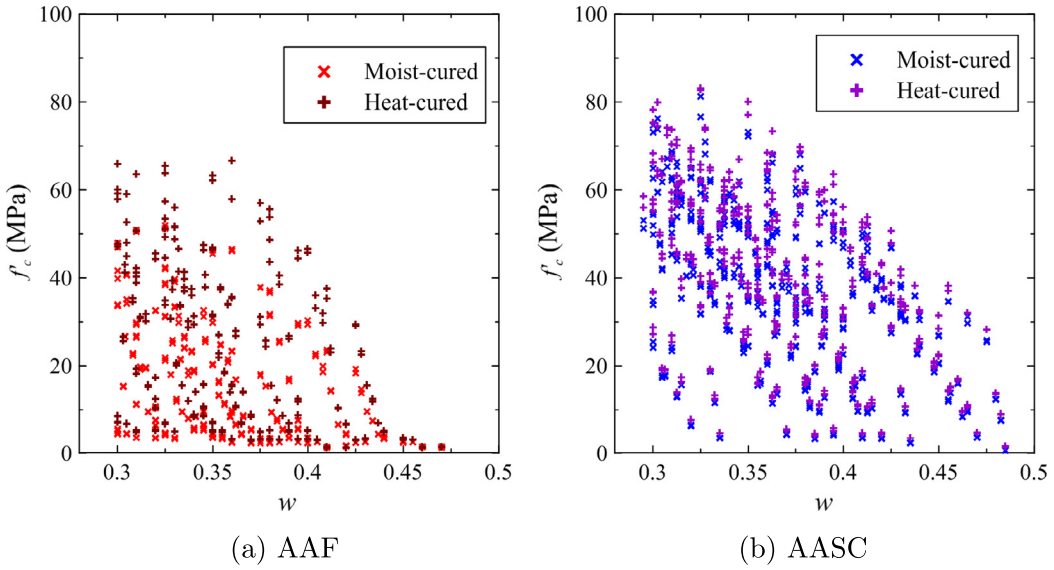

Fig. 5. Compressive strength f'_c vs. free water-to-binder ratio w.

$$f'_c = 10.08 - 6.930T + 1.798N - 5.071S + 6.820m - 37.51s + 3.500TN + 1.778NS - 0.2023S^2 \quad (6)$$

$$f'_c = -46.40 - 7.714T + 57.47N - 250.2S + 277.9m - 30.08s + 3.166TN + 0.4750TS + 67.12NS + 84.92mS - 16.24N^2 - 23.02S^2 - 93.79m^2 - 5.045N^2S + 1.644NS^2 + 1.329N^3 + 0.0567S^3 \quad (7)$$

Due to the number of regressors, it is impossible to plot the above equations for visualization purposes or for evaluation of goodness of fit. The latter can be instead achieved by plotting the predicted compressive strength f'_c against the measured compressive strength f'^*_c. It is useful to compute a linear regression correlating the two and to solve for the corresponding coefficient of correlation (R^2). If the fit is very good, the resulting regression should have a slope near 1, an intercept near zero, and a coefficient of correlation near 1. This method of evaluation provides an estimation of goodness of fit, but gives no information about efficiency due to the lack of an overfitting penalty.

The predicted compressive strength f'_c according to the proposed model Eqs. (3)–(7) is plotted against the average compressive strength of each batch of AAF concrete in Figs. 6–10, respectively. The linear regression line and coefficient of correlation (R^2) are shown on each figure. In general, as the model order increases so does the goodness of fit. This is indicated by the slope of the regression line and the coefficient of correlation approaching unity. Even with the most complex model (the cubic model of Eq. (7)), the coefficient of correlation is a mere 0.93. While the cubic model is certainly the best of the models presented here in terms of goodness of fit, it is by no means exceptional.

Some ordinate values are negative in each case, meaning that the predicted compressive strength is negative while the measured compressive strength is obviously not. This is problematic from a theoretical standpoint. From a practical standpoint it is inconsequential because it only occurs for specimens with very low compressive strength ($f'^*_c < 5$ MPa). Also worthy of mention is the marked heteroscedasticity of the data presented in Figs. 6–10 The aberrant distribution of residuals in Figs. 6–10 are also worthy of mention. An underlying assumption of regression modeling is

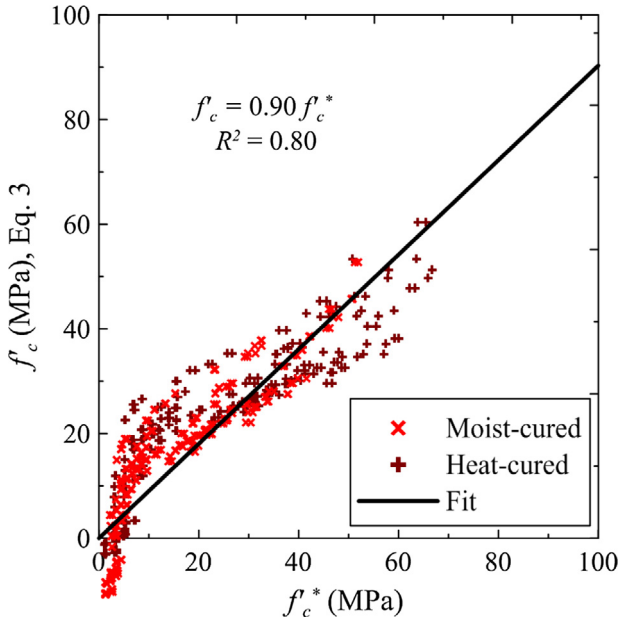

Fig. 6. Predicted compressive strength f'_c vs. measured compressive strength f'^*_c for AAF (Linear without interactions).

that the data are homoscedastic, or that the variance is constant throughout the range of measurement. This suggests that none of the models presented here for strength prediction in AAF concrete are entirely appropriate, although the data seem to become more homoscedastic with increasing model order. With some of the higher-order models (e.g., the cubic model of Eq. (7) and Fig. 10), only the heat-cured strength data are heteroscedastic.

The efficiency of the proposed models can also be evaluated numerically using the BIC as defined by Eq. (1). A comparison of model order, number of model terms, and BIC for the proposed models is given in Table 3. Even with a heavy penalty for overfitting, the optimal model for compressive strength prediction in sodium silicate-activated fly ash is shown numerically to be the cubic model of Eq. (7). With 17 terms in five variables, this is arguably not an economical predictive model. Furthermore, the difference in BIC numbers is only slight, representing a 9% improvement in BIC over the next best models, both of which

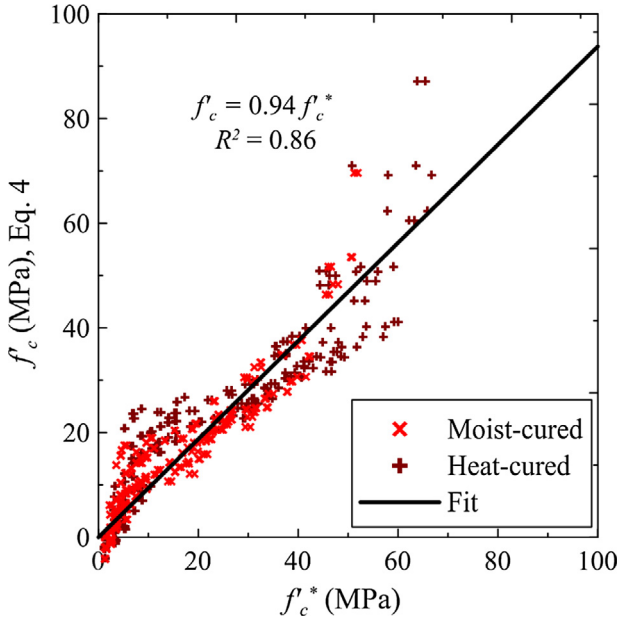

Fig. 7. Predicted compressive strength f'_c vs. measured compressive strength f'^*_c for AAF (Linear with interactions).

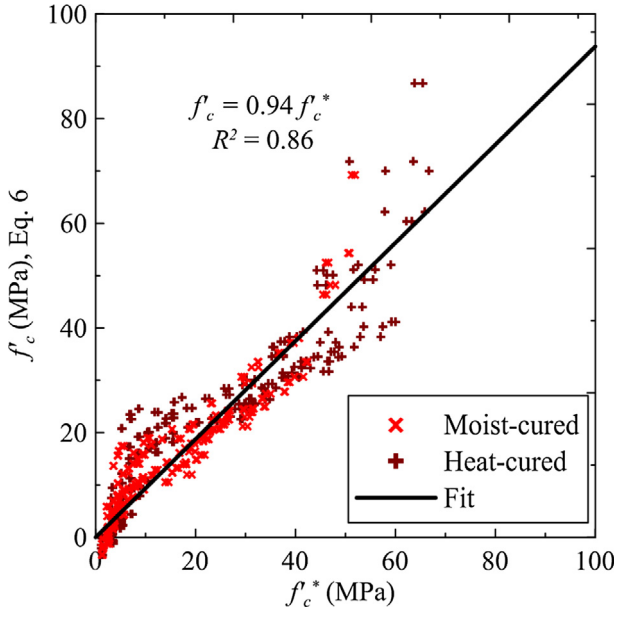

Fig. 9. Predicted compressive strength f'_c vs. measured compressive strength f'^*_c for AAF (Quadratic with interactions).

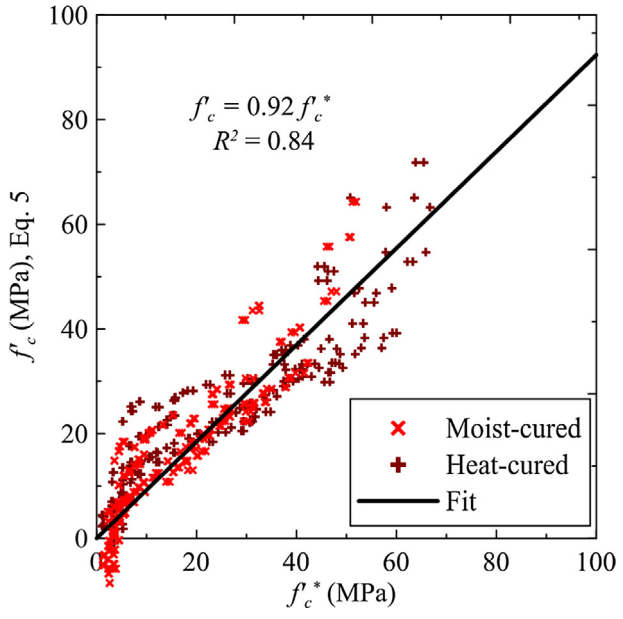

Fig. 8. Predicted compressive strength f'_c vs. measured compressive strength f'^*_c for AAF (Quadratic without interactions).

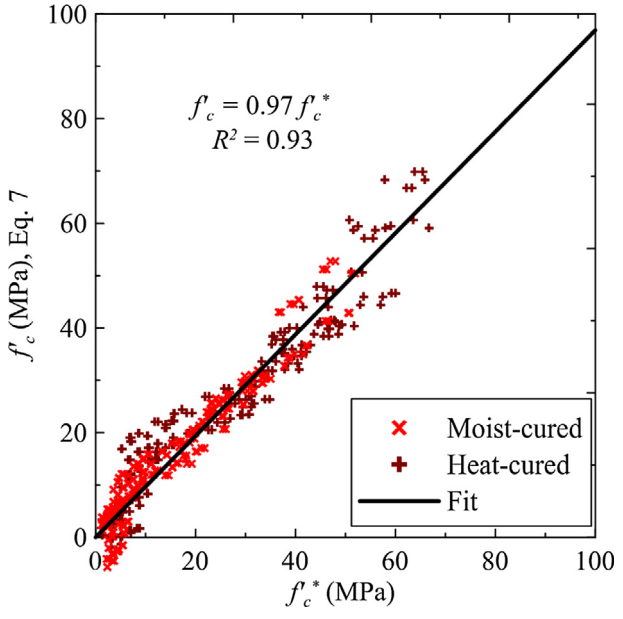

Fig. 10. Predicted compressive strength f'_c vs. measured compressive strength f'^*_c for AAF (Cubic with interactions).

had half the number of terms, and a 14% improvement over the simplest model with one-third the number of terms. Nevertheless, the evidence shown in Fig. 10 suggests that the cubic model provides the best prediction of compressive strength, and the BIC number suggests that the same model provides the most efficient prediction of compressive strength. Overall, none of the models presented here predict the compressive strength extremely well or with extreme efficiency.

Table 3
Model ranking for compressive strength of AAF concrete.

Model	Equations	Terms	BIC
Linear without interactions	(3)	6	3517
Linear with interactions	(4)	9	3314
Quadratic without interactions	(5)	8	3411
Quadratic with interactions	(6)	9	3314
Cubic with interactions	(7)	17	3018

4.2.2. AASC concrete

In the same manner, five models of increasing order were fit to predict the compressive strength of AASC concrete. These are given by Eqs. (8)–(12) for model classes 1–5, respectively. Similar conclusions may be drawn from these models as were drawn from those for AAF concrete. As with the proposed models for the compressive strength of AAF concrete, those for AASC concrete all include terms for curing condition, sodium oxide concentration, silica

concentration, and silica modulus. All but the highest order model (the cubic model of Eq. (12)) include terms for solution-to-binder ratio, while Eq. (12) includes terms for the free water-to-binder ratio. None of the models include terms for both. Regardless of model order, this again suggests that while three terms describing the activator composition are necessary, only one describing the water content is necessary. Evidence suggests that the solution-to-binder ratio provides a better prediction of compressive strength than the free water-to-binder ratio.

It is interesting to note the similarity in coefficients between models. The coefficient on the term T is identical for all but Eq. (11). Moving from lower-order models to higher-order models did not significantly alter the lower-order terms. In other words: Fitting a higher-order model simply adds higher-order terms and adjusts coefficients. In contrast, fitting higher order models for AAF concrete resulted in different lower-order terms in many cases. This suggests that, while the algorithm struggled to produce a well-fitting model for AAF concrete, even the lower-order models for AASC concrete fit reasonably well.

$$f'_c = 10.71 + 2.545T + 7.300N + 1.330S + 11.09m - 49.05s \quad (8)$$

$$f'_c = -10.14 + 2.545T + 5.202N + 13.32S + 13.93m - 15.47s - 0.2814NS - 2.137mS - 8.873Ss \quad (9)$$

$$f'_c = -37.48 + 2.545T + 4.524N + 5.141S + 28.76m + 116.5s + 0.3130N^2 - 0.2743S^2 - 5.000m^2 - 181.7s^2 \quad (10)$$

$$f'_c = -13.41 + 1.604T + 4.594N + 8.270S + 29.17m - 17.61s + 0.2366TS - 8.259Ss + 0.3177N^2 - 0.2231S^2 - 5.099m^2 \quad (11)$$

$$f'_c = 21.29 + 2.545T - 18.05N + 19.06S - 24.12w - 5.815Ss + 4.947N^2 - 1.297S^2 - 0.3530N^3 + 0.0343S^3 \quad (12)$$

The predicted compressive strength f'_c according to the proposed model Eqs. (8)–(12) is plotted against the average compressive strength f'^*_c each batch of AASC concrete in Figs. 11–15, respectively. In the same manner as before, the linear regression line and coefficient of correlation are plotted on the same figures. The overall goodness of fit was much improved over the predictive models for AAF concrete. The slope of the regression line in each case was very near unity. For all but the simplest model (the linear model of Eq. (8) and Fig. 11), the coefficient of correlation was 95% or better. The higher-order model Eqs. (9)–(12) all offer excellent goodness of fit, and it is impossible to select any one that is better than the others based on this information.

A numerical analysis of model efficiency using BIC is presented in Table 4. The BIC numbers for AASC models are almost twice those for AAF models, which is a result of the increased sample size (recall that BIC$= k\ln n - 2\hat{\ell}$, where n is the sample size, and that BIC is minimized). The number of model terms was generally less in AASC models than in AAF models (e.g., 20 terms in the cubic model for AAF concrete vs. 10 in that for AASC concrete). The optimal model according to the BIC comparison was the quadratic model with interactions of Eq. (11), although the quadratic model without interactions of Eq. (10) was a very close second and included one fewer term. Either model represented about a 18% improvement in BIC over the linear model of Eq. (8). Again, there is some value in considering the validity of a small improvement in model criterion at the cost of a twofold increase in model complexity. Nonetheless, the analysis in Figs. 11,12 suggests that the higher-order models of Eqs. (9)–(12) were much better than the linear model without interactions of Eq. (8). As such, either quadratic model with or without interactions is a clear choice.

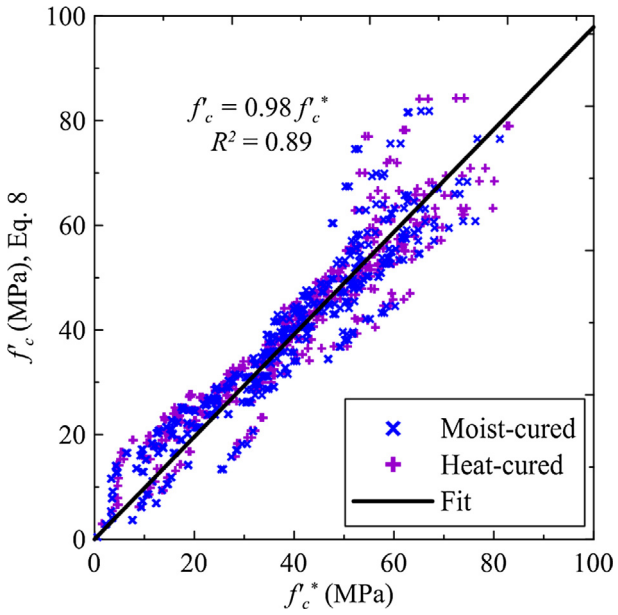

Fig. 11. Predicted compressive strength f'_c vs. measured compressive strength f'^*_c for AASC (Linear without interactions).

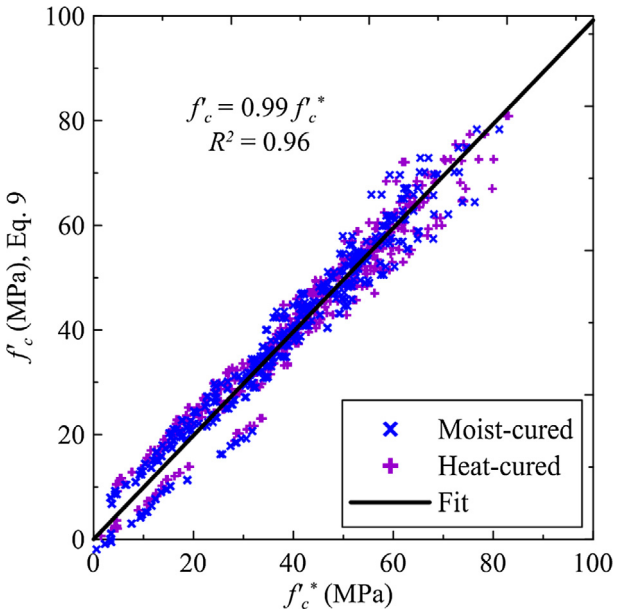

Fig. 12. Predicted compressive strength f'_c vs. measured compressive strength f'^*_c for AASC (Linear with interactions).

5. Summary

A comprehensive experimental study of the effects of curing condition, sodium oxide dosage, silica dosage, silica modulus, solution-to-binder ratio and water-to-binder ratio on the compressive strength of sodium silicate activated fly ash and slag cement concrete was performed. The individual effects of each variable were investigated. For both binders and within the ranges investigated here, the compressive strength increased with sodium

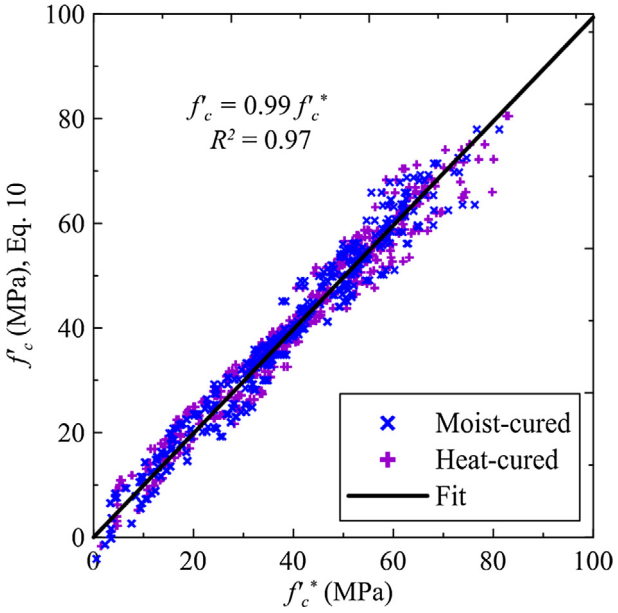

Fig. 13. Predicted compressive strength f'_c vs. measured compressive strength f'^*_c for AASC (Quadratic without interactions).

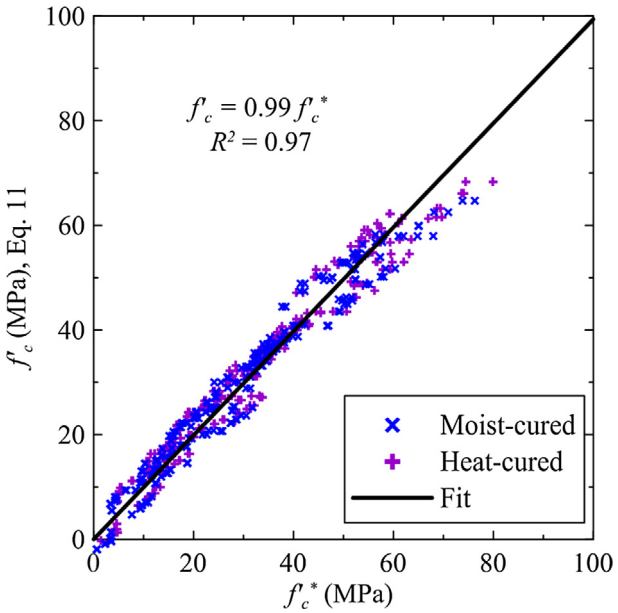

Fig. 14. Predicted compressive strength f'_c vs. measured compressive strength f'^*_c for AASC (Quadratic with interactions).

oxide dosage and silica dosage. Similarly, the compressive strength decreased with free water-to-binder ratio. The effects of silica modulus and solution-to-binder ratio were mixed and less clear.

Mathematical models were developed to predict the compressive strength based on the aforementioned variables. Models were determined by stepwise regression analysis and ranked by Bayesian Information Criterion. A simple linear model can predict the compressive strength of alkali-activated slag cement concrete with reasonable accuracy. A quadratic model can do the same with excellent accuracy and efficiency. The best model for the compressive strength of sodium silicate-activated slag cement concrete was quadratic function of the curing condition, sodium oxide dosage, silica dosage, silica modulus, and solution-to-binder ratio. This

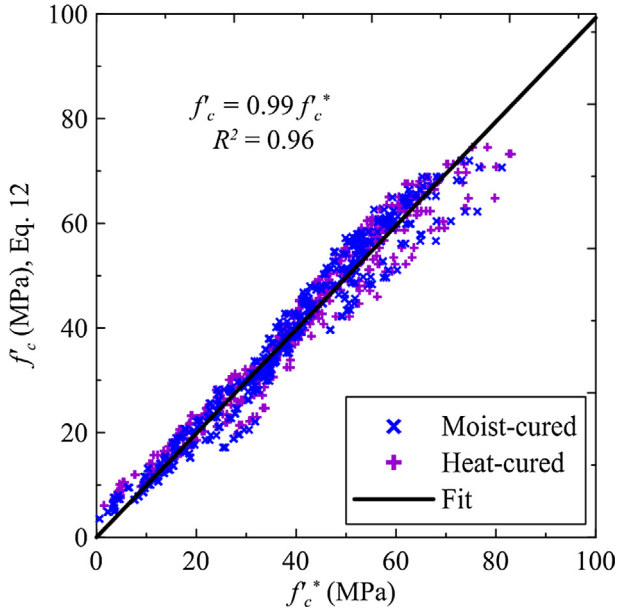

Fig. 15. Predicted compressive strength f'_c vs. measured compressive strength f'^*_c for AASC (Cubic with interactions).

Table 4
Comparison of models for compressive strength of AASC concrete.

Model	Equation	Terms	BIC
Linear without interactions	(8)	6	5565
Linear with interactions	(9)	9	4787
Quadratic without interactions	(10)	10	4584
Quadratic with interactions	(11)	11	4560
Cubic with interactions	(12)	10	4697

model performed very well with and without the inclusion of interaction effects. The compressive strength of sodium silicate-activated fly ash concrete was difficult to predict even using a cubic function with twenty terms and the same predictors. The most efficient models for both binders did not include terms for the free water-to-binder ratio, suggesting that the solution-to-binder ratio is more important in predicting compressive strength. Meanwhile, three terms describing the activator concentration (sodium oxide dosage, silica dosage, and silica modulus) were necessary for accurate prediction of compressive strength.

Acknowledgment

The authors gratefully acknowledge the financial support from the University Transportation Research Center, Region 2 (UTRC2) through the University Transportation Centers program and from the National Science Foundation under CMMI Award No. 1055641. Any opinions, findings, and conclusions or recommendations expressed in this article are those of the authors and do not necessarily reflect the views of UTRC2 or of the National Science Foundation.

References

[1] H. Kühl. Slag cement and process of making the same., October 1908. US Patent 900, 939.
[2] P. Duxson, J.L. Provis, G.C. Lukey, J.S.J. Van Deventer, The role of inorganic polymer technology in the development of green concrete, Cem. Concr. Res. 37 (12) (2007) 1590–1597.
[3] B.C. McLellan, R.P. Williams, J. Lay, A. Van Riessen, G.D. Corder, Costs and carbon emissions for geopolymer pastes in comparison to ordinary portland cement, J. Cleaner Prod. 19 (9) (2011) 1080–1090.

[4] M. Jiang, X. Chen, F. Rajabipour, C.T. Hendrickson, Comparative life cycle assessment of conventional, glass powder, and alkali-activated slag concrete and mortar, J. Infrastruct. Syst. 20 (4) (2014) 04014020.
[5] S.D. Wang, K.L. Scrivener, P.L. Pratt, Factors affecting the strength of alkali-activated slag, Cem. Concr. Res. 24 (6) (1994) 1033–1043.
[6] A.M. Fernández-Jiménez, J.G. Palomo, F. Puertas, Alkali-activated slag mortars: mechanical strength behaviour, Cem. Concr. Res. 29 (8) (1999) 1313–1321.
[7] T. Bakharev, J.G. Sanjayan, Y.B. Cheng, Alkali activation of australian slag cements, Cem. Concr. Res. 29 (1) (1999) 113–120.
[8] A.M. Fernández-Jiménez, F. Puertas, Effect of activator mix on the hydration and strength behaviour of alkali-activated slag cements, Adv. Cem. Res. 15 (3) (2003) 129–136.
[9] C. Duran Atiş, C. Bilim, Ö. Çelik, O. Karahan, Influence of activator on the strength and drying shrinkage of alkali-activated slag mortar, Constr. Build. Mater. 23 (1) (2009) 548–555.
[10] E. Douglas, A. Bilodeau, V.M. Malhotra, Properties and durability of alkali-activated slag concrete, ACI Mater. J. 89 (5) (1992).
[11] F.G. Collins, J.G. Sanjayan, Workability and mechanical properties of alkali activated slag concrete, Cem. Concr. Res. 29 (3) (1999) 455–458.
[12] A.R. Brough, A. Atkinson, Sodium silicate-based, alkali-activated slag mortars: Part I. Strength, hydration and microstructure, Cem. Concr. Res. 32 (6) (2002) 865–879.
[13] T. Bakharev, J.G. Sanjayan, Y.B. Cheng, Effect of elevated temperature curing on properties of alkali-activated slag concrete, Cem. Concr. Res. 29 (10) (1999) 1619–1625.
[14] V. Živica, Effects of type and dosage of alkaline activator and temperature on the properties of alkali-activated slag mixtures, Constr. Build. Mater. 21 (7) (2007) 1463–1469.
[15] E. Altan, S.T. Erdoğan, Alkali activation of a slag at ambient and elevated temperatures, Cem. Concr. Compos. 34 (2) (2012) 131–139.
[16] S. Aydn, B. Baradan, Mechanical and microstructural properties of heat cured alkali-activated slag mortars, Mater. Des. 35 (2012) 374–383.
[17] S.A. Bernal, R.M. de Gutiérrez, A.L. Pedraza, J.L. Provis, E.D. Rodriguez, S. Delvasto, Effect of binder content on the performance of alkali-activated slag concretes, Cem. Concr. Res. 41 (1) (2011) 1–8.
[18] J.G.S. Van Jaarsveld, J.S.J. Van Deventer, Effect of the alkali metal activator on the properties of fly ash-based geopolymers, Ind. Eng. Chem. Res. 38 (10) (1999) 3932–3941.
[19] D. Li, Y. Chen, J. Shen, J. Su, X. Wu, The influence of alkalinity on activation and microstructure of fly ash, Cem. Concr. Res. 30 (6) (2000) 881–886.
[20] A.M. Fernández-Jiménez, A. Palomo, C. Lopez-Hombrados, Engineering properties of alkali-activated fly ash concrete, ACI Mater. J. 103 (2) (2006) 106–112.
[21] D. Panias, I.P. Giannopoulou, T. Perraki, Effect of synthesis parameters on the mechanical properties of fly ash-based geopolymers, Colloids Surf., A 301 (1) (2007) 246–254.
[22] G. Kovalchuk, Ana Fernández-Jiménez, A. Palomo, Alkali-activated fly ash: Effect of thermal curing conditions on mechanical and microstructural development–Part II, Fuel 86 (3) (2007) 315–322.
[23] G. Kovalchuk, A. Fernández-Jiménez, A. Palomo, Alkali-activated fly ash. Relationship between mechanical strength gains and initial ash chemistry, Mater. Constr. 58 (291) (2008) 35–52.
[24] M. Criado, Ana Fernández-Jiménez, A. Palomo, Alkali activation of fly ash. part iii: Effect of curing conditions on reaction and its graphical description, Fuel 89 (11) (2010) 3185–3192.
[25] A.S. De Vargas, D.C.C. Dal Molin, A.C.F. Vilela, F.J. Da Silva, B. Pavão, H. Veit, The effects of Na_2O/SiO_2 molar ratio, curing temperature and age on compressive strength, morphology and microstructure of alkali-activated fly ash-based geopolymers, Cem. Concr. Compos. 33 (6) (2011) 653–660.
[26] E. Deir, B.S. Gebregziabiher, S. Peethamparan, Influence of starting material on the early age hydration kinetics, microstructure and composition of binding gel in alkali activated binder systems, Cem. Concr. Compos. 48 (2014) 108–117.
[27] A. Palomo, M.W. Grutzeck, M.T. Blanco, Alkali-activated fly ashes: A cement for the future, Cem. Concr. Res. 29 (8) (1999) 1323–1329.
[28] F. Puertas, S. Martnez-Ramrez, S. Alonso, T. Vazquez, Alkali-activated fly ash/slag cements: Strength behaviour and hydration products, Cem. Concr. Res. 30 (10) (2000) 1625–1632.
[29] J.L. Provis, C.Z. Yong, P. Duxson, J.S.J. van Deventer, Correlating mechanical and thermal properties of sodium silicate-fly ash geopolymers, Colloids Surf., A 336 (1) (2009) 57–63.
[30] X. Guo, H. Shi, W.A. Dick, Compressive strength and microstructural characteristics of class c fly ash geopolymer, Cem. Concr. Compos. 32 (2) (2010) 142–147.
[31] D. Bondar, C.J. Lynsdale, N.B. Milestone, N. Hassani, Oxygen and chloride permeability of alkali-activated natural pozzolan concrete, ACI Mater. J. 109 (1) (2012) 53–61.
[32] K.L. Aughenbaugh, T. Williamson, M.C.G. Juenger, Critical evaluation of strength prediction methods for alkali-activated fly ash, Mater. Struct. 48 (3) (2015) 607–620.
[33] Steven H. Kosmatka, Beatrix Kerkhoff, William C. Panarese, Design and control of concrete mixtures, Portland Cem. Assoc. (2011).
[34] R.J. Thomas, S. Peethamparan, Alkali-activated concrete: Engineering properties and stress-strain behavior, Constr. Build. Mater. 93 (2015) 49–56.
[35] R.J. Thomas, S. Peethamparan. Effect of specimen size and curing condition on the compressive strength of alkali-activated concrete. Transp. Res. Rec., In Press.
[36] R.J. Thomas, A. Howe, S Peethamparan, Alkali–activated cement free concrete: Development of practical mixtures for construction, in: Proceedings of the 93rd Annual Meeting of the Transportation Research Board. Transportation Research Board, 2014.
[37] Martin J. Gardner, Douglas G. Altman, Confidence intervals rather than p values: Estimation rather than hypothesis testing, Br. Med. J. (Clin. Res. Ed.) 292 (6522) (1986) 746–750.
[38] James O. Berger, Thomas Sellke, Testing a point null hypothesis: The irreconcilability of p values and evidence, J. Am. Stat. Assoc. 82 (397) (1987) 112–122.